The Dynamics of Periodically Forced Prolate Spheroids in a Quiescent Newtonian Fluid with Weak Inertia

Priyank Vijaya Kumar

Indian Institute of Technology Madras Department of Metallurgical and Materials Engineering, Chennai - 600 036, India

Abstract

The effects of convective and unsteady inertia on the dynamics of periodically forced neutrally buoyant prolate spheroids in a quiescent Newtonian fluid medium, at low Reynolds numbers have been modeled. The resulting nonlinear equations have been solved using appropriate numerical methods. Several tests including a perturbation analysis are performed to validate results. A preferred direction, which is identified as the initial direction of motion, is observed that manifests itself in the properties of the solution. Results of the behaviour of various parameters with respect to the Reynolds number, aspect ratio of the spheroid and the amplitude of the periodic force are presented. The results are technologically important as they may lead to insights in the development of active dampeners and smart fluids.

Keywords: Low Reynolds Number, Quiescent Fluid, Prolate Spheroid, Aspect Ratio, Periodic Force, Inertial Effects

1. Introduction

Suspensions of solid particles are encountered both as raw materials and as intermediates in a large number of industries such as printing and paper making, petroleum, pharmaceuticals, and food processing. Suspension rheology leads to insights which may lead to better control of fluid stress deformation behaviour and hence may lead to appropriate changes in processing parameters. In most situations, the particles tend to be non-spherical or even irregularly shaped, the suspension rheology then being sensitive to the orientation distribution of the suspended particles. The motion of non-spherical particles in shear flows at vanishingly small Reynolds numbers has been studied theoretically for a long time and is summarized by Leal[1]. It has, in fact been known since the work of Jeffery[2] and later Bretherton[3] at zero Reynolds numbers, that in the absence of inertia, an axisymmetric particle in a simple shear flow rotates periodically in one of an infinite single–parameter family of closed 'Jeffery' orbits. The particular orbit adopted by the particle, in the absence of hydrodynamic interactions, Brownian motion, etc. depends on the initial conditions, rendering the inertialess limit indeterminate. Subramanian and Koch[4] considered both particle and fluid inertia as a possible mechanism acting to remove this indeterminancy. They developed solutions for aspect ratios close to unity. Hence, their analysis captures the leading order effect of the deviation from sphericity on the particle orientational motion. They found that for the neutrally buoyant case, the inertia of the suspending fluid causes a prolate spheroid to drift toward an axial spin about the vorticity axis of the ambient simple shear.

Ramamohan and coworkers[5,6] have been studying the dynamics and rheology of periodically forced suspensions for a period of about two decades. The class of problems they have studied has fundamental importance and technological potential. This class of problems is one of the simplest physically realizable fluid dynamical systems that can show chaos at the level of the individual particle. It has been shown that there exists a chaotic parametric regime, in the dynamics of periodically forced spheroidal particles in a simple shear flow[7]. This chaotic dynamics can be controlled by controlling the system parameters[8]. These results restricted to zero Reynolds numbers and simple shear flow have been summarized by Asokan et al[5].

Recently Ramamohan et al[6], have studied the dynamics and rheology of a dilute suspension of neutrally buoyant periodically forced spherical particles in a quiescent Newtonian fluid at low Reynolds numbers. Since most realistic suspensions have non-spherical shapes, The results reported in this work show that data based on simulations with spheres may need to be modified before they can be

applied to realistic situations. Hence, in this paper, these results are extended to prolate spheroidal particle suspensions.

Table 1. List of Symbols.

F^H	Hydrodynamic force on particle
F_s^H	Steady force drag on particle
F^{Ext}	External force on particle
Φ	Stokes resistance tensor
M	Transformation tensor defined such that $u_0=MU_s$
U_s	Slip velocity of the particle
U^∞	Velocity of the fluid
U_p	Velocity of the particle
Y_s	Displacement of the particle
Re	Reynolds number
Sl	Strouhal number
U_C	Characteristic velocity of the particle
F_0	Amplitude of the periodic force
Re_F	Scaled amplitude of the periodic force
ω	Frequency of oscillation
a	Characteristic particle dimension, semi-major axis of the spheroid
b	Semi-minor axis of the spheroid
e	Eccentricity of the spheroid
m_p	Mass of the particle
ρ	Density of the particle
ν	Kinematic viscosity of the fluid
μ	Viscosity of the fluid
Y_{pmean}	Mean displacement of the particle

2. The Hydrodynamic Force Expression for an Arbitrary Shaped Particle

Lovalenti and Brady[9] give the expression for the required hydrodynamic force on an arbitrary shaped particle, in the long time limit at low Reynolds numbers.

This is the most rigorous equation which results in an ODE at low but non-zero Re. The reciprocal theorem has been used to obtain the following expression. The details of the derivation can be found in Lovalenti and Brady[9].

$$\boldsymbol{F}^H(t) = ReSlV_P\dot{\boldsymbol{U}}^\infty(t) + \boldsymbol{F}_S^H(t) - ReSl\left[6\pi\boldsymbol{\phi}.\boldsymbol{\phi}.\boldsymbol{\phi} + \lim_{R\to\infty}\left(\int_{V_F(R)}\boldsymbol{M}^T.\boldsymbol{M}dV - \frac{9\pi}{2}\boldsymbol{\phi}.\boldsymbol{\phi}R\right)\right].\dot{\boldsymbol{U}}_S(t) + \frac{3}{8}\left(\frac{ReSl}{\pi}\right)^{\frac{1}{2}}\left\{\int_{-\infty}^{t}\left[\frac{2}{3}\boldsymbol{F}_S^{H\parallel}(t) - \left\{\frac{1}{|A|^2}\left(\frac{\pi^{\frac{1}{2}}}{2|A|}\mathrm{erf}(|A|) - \exp(-|A|^2)\right)\right\}\boldsymbol{F}_S^{H\parallel}(s) + \frac{2}{3}\boldsymbol{F}_S^{H\perp}(t) - \left\{\exp(-|A|^2) - \frac{1}{2|A|^2}\left(\frac{\pi^{\frac{1}{2}}}{2|A|}\mathrm{erf}(|A|) - \exp(-|A|^2)\right)\right\}\boldsymbol{F}_S^{H\perp}(s)\right] \times \frac{2ds}{(t-s)^{1/2}}\right\}.\boldsymbol{\phi} - Re\lim_{R\to\infty}\int_{V_F(R)}(\boldsymbol{u}_0.\nabla\boldsymbol{u}_0 - \boldsymbol{U}_s(t).\nabla\boldsymbol{u}_0).\boldsymbol{M} + O(ReSl) + O(Re) \quad (1)$$

Here, $\boldsymbol{U}_s = \boldsymbol{U}_p - \boldsymbol{U}^\infty$ is the slip velocity of the particle. $\boldsymbol{U}_p$ is the velocity of the particle. $\boldsymbol{U}_s$ has been non-dimensionalized by $\boldsymbol{U}_c$. The acceleration terms $\dot{\boldsymbol{U}}_S$ and $\dot{\boldsymbol{U}}^\infty$ are non- dimensionalized by $\omega\boldsymbol{U}_c$, where $1/\omega$ is the characteristic timescale. $\boldsymbol{U}^\infty$ is the velocity of the fluid as $r\to\infty$. *Re* is the Reynolds number, defined as $Re=U_ca/\nu$ based on a characteristic particle slip velocity, $\boldsymbol{U}_c$, '*a*' denotes the characteristic particle dimension, in this case the semi-major axis and ν is the kinematic viscosity of the fluid. $\boldsymbol{F}_S^H = -6\pi(\boldsymbol{\phi}.\boldsymbol{U}_S)$, $\boldsymbol{F}_S^{H\parallel} = -6\pi(\boldsymbol{\phi}.\boldsymbol{U}_S).(\boldsymbol{pp})$, $\boldsymbol{F}_S^{H\perp} = -6\pi(\boldsymbol{\phi}.\boldsymbol{U}_S).(\boldsymbol{\delta}-\boldsymbol{pp})$, where $\boldsymbol{\delta}$ is the idem tensor of order 2 and unit vector $\boldsymbol{p} = \frac{\boldsymbol{Y}_S(t)-\boldsymbol{Y}_S(s)}{|\boldsymbol{Y}_S(t)-\boldsymbol{Y}_S(s)|}$, here $\boldsymbol{Y}_s(t)$-$\boldsymbol{Y}_s(s)$ is the integrated displacement of the particle relative to the fluid from time *s* to the current time *t*. $\boldsymbol{F}^H$ is scaled by $\mu a\boldsymbol{U}_c$. *Sl* is the Strouhal number, V_P is the scaled particle volume and '*A*' is given by

$$A = \frac{Re}{2}\left(\frac{t-s}{ReSl}\right)^{\frac{1}{2}}\left(\frac{\boldsymbol{Y}_S(t)-\boldsymbol{Y}_S(t)}{t-s}\right)$$

The first term on the right hand side of the differential expression is due to an accelerating reference frame. The second is the pseudo-steady Stokes drag. The third is called the acceleration reaction, similar to the added mass. The fourth term represents the unsteady Oseen correction, which replaces the 'Basset memory integral' in the long time limit at finite Reynolds number. The last integral contributes a lift force, i.e. a force perpendicular to the slip velocity. Note that the expression is valid up to order *Re* and order *ReSl*.

The acceleration reaction term (I_1=int-xx in Table-2) is computed using the expressions given by Pozrikidis[10] and

Chwang and Hu[11]. The expression for the Stokes resistance tensor (Φ) in its dimensionless form is given by

$$\boldsymbol{\phi} = \frac{8e}{3}(\boldsymbol{a}) \qquad (2)$$

Here, e is the eccentricity of the spheroid and a is the diagonal matrix mentioned in Chwang and Hu[11].

Table 2. Computed Values of the Diagonal Matrix Representing the Acceleration Reaction Term.

Aspect Ratio (a/b)	int-xx	int-yy	int-zz
2	0.7261	1.3266	1.3897
3	0.3510	0.7915	0.8378
4	0.2288	0.5447	0.5828
5	0.1624	0.3963	0.4292
6	0.1242	0.3009	0.3301
7	0.0998	0.2353	0.2619
8	0.0830	0.1872	0.2124
9	0.0682	0.1487	0.1723
10	0.0591	0.1208	0.1430

In the current work, only one dimensional motion of the particle is considered. The translation is along this major axis of the spheroid and hence is symmetric with respect to the particle. The lift force term is neglected as it contributes only to a force in the perpendicular direction and is zero in this case. This has been verified in these computations.

3. Solving The Differential Equation

After obtaining suitable expressions and values for different aspect ratios, the dynamics of a spheroidal particle were determined.

3.1 Formulation of the Problem

The force equation (1) given by Lovalenti and Brady for an arbitrary shaped particle undergoing an arbitrary time-dependent motion at low Reynolds numbers, in the long time limit is considered. In this case a neutrally buoyant prolate spheroid in an infinite body of quiescent fluid is considered, as well as the effects of an external periodic force acting on the spheroid along the x-axis.

The governing expression for the unidirectional motion of a spheroid in a quiescent fluid medium is obtained, starting with zero velocity at time $t=0$, with $\boldsymbol{U}_s = \boldsymbol{U}_P - \boldsymbol{U}^{\infty}$ where $\boldsymbol{U}_p$ is the velocity of the particle, scaled with respect to the size of the particle and the frequency of the external periodic force, ω, i.e. we take $\boldsymbol{U}_c = a\omega$ and $\boldsymbol{U}^{\infty} = 0$.

Note that there exists a singularity (point at which the intergral term becomes indeterminate) at $s=t$. Hence, in order to avoid this singularity, the integral in the interval $[0,\ t-\epsilon]$ is evaluated, where ϵ is chosen to be a very small number. Note that in the limit $s \to t$, the integral converges to a finite limit and hence the value of the integral in the range $s=t-\epsilon$ to $s=t$ is negligible. Under these conditions, equation (1) reduces to

$$\boldsymbol{F}^H(t) = -6\pi(cof)\boldsymbol{U}_P(t) - ReSl(I_1)\dot{\boldsymbol{U}}_s(t) + \frac{3}{8}\left(\frac{ReSl}{\pi}\right)^{\frac{1}{2}}(cof)^2\left\{\int_0^{t-\epsilon}\left\{\frac{1}{|A|^2}\left(\frac{\pi^{\frac{1}{2}}}{2|A|}\mathrm{erf}(|A|) - \exp(-|A|^2)\right)\right\}\frac{12\pi\boldsymbol{U}_P(s)}{(t-s)^{3/2}}ds + 16\pi\boldsymbol{U}_P(t)\left[\frac{1}{\sqrt{t}} - \frac{1}{\sqrt{\epsilon}}\right]\right\} \qquad (3)$$

Here, $cof = \frac{8}{3}ea_{11}$ and I_1 is the computed acceleration term.

Now, the equation of motion for a neutrally buoyant particle immersed in a liquid is given by

$$\frac{m_P\dot{\boldsymbol{U}}_P(t)}{\mu a^2\omega} = \boldsymbol{F}^{ext}(t) + \boldsymbol{F}^H(t) \qquad (4)$$

The periodic force $\boldsymbol{F}^{ext}(t) = \boldsymbol{F}_0\sin(t)$ is used, where time has been scaled with respect to the frequency of the external periodic force. The following equations for the displacement and velocity of the particle using Newtons second law of motion were obtained.

$$\frac{d\boldsymbol{Y}_P}{dt} = \boldsymbol{U}_P \qquad (5)$$

$$\frac{d\boldsymbol{U}_P}{dt} = \frac{1}{Re'}\left[Re_F\sin(t) - 6\pi(cof)\boldsymbol{U}_P + \frac{3}{8}\left(\frac{ReSl}{\pi}\right)^{\frac{1}{2}}(cof)^2(P_1+Q_1)\right] \qquad (6)$$

where,

$$Re' = \frac{4\pi}{3}\left(\frac{b}{a}\right)^2 Re + (I_1)ReSl\,,\quad Re_F = \frac{F_0}{\mu a^2\omega}\,,\quad Re = \frac{\rho a^2\omega}{\mu}$$

Here, a is the characteristic particle dimension, ρ is the density of the particle and μ is the fluid viscosity.

$$P_1 = \int_0^{t-\epsilon}\left\{\frac{1}{|A|^2}\left(\frac{\pi^{\frac{1}{2}}}{2|A|}\mathrm{erf}(|A|) - \exp(-|A|^2)\right)\right\}\frac{12\pi U_P(s)}{(t-s)^{3/2}}ds$$

$$Q_1 = 16\pi\boldsymbol{U}_P(t)\left[\frac{1}{\sqrt{t}} - \frac{1}{\sqrt{\epsilon}}\right]$$

3.2 Numerical Procedure

The differential equation was solved using a time-stepping finite difference routine. In order to accommodate the nonlinear integral term, the product trapezoidal rule[12] was implemented. The value of ε was chosen to be equal to 0.0001. Further decrease in its value did not result in any significant changes of the velocity and displacement values.

Two sets of data points, 150000 and 350000, taken at an interval of 0.0001 in both the dimensionless velocity and dimensionless position were generated. Further increase in resolution did not yield any significant difference in the results.

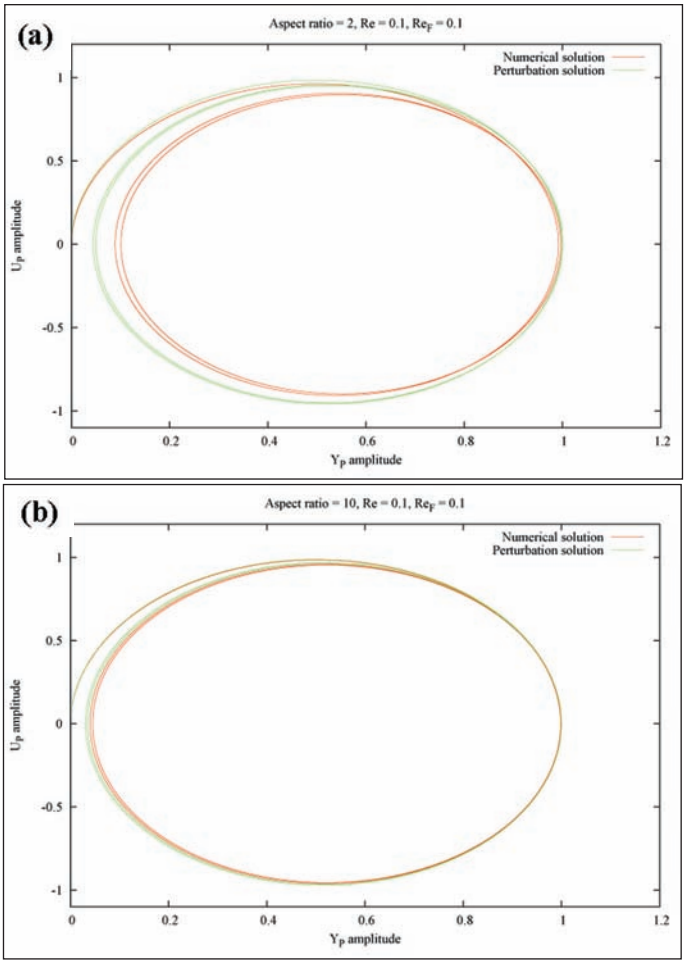

Figure 1. The phase plot obtained compares the numerical solution with the perturbed solution. This has been seen for Re=0.1, ReF=0.1, aspect ratio=2(a) and 10(b). The match is very good in the second case owing to reduced inertial effects at higher aspect ratios and hence reduced nonlinearity.

3.3 Tests

Several tests were performed in order to validate the results. They are listed below.

3.3.1 Test 1 Perturbation Analysis

Perturbation solutions were obtained in order to validate our results for small Re. The Taylor series expansion for the nonlinear integral term was used. One important aspect to be noted is that the expression given for an arbitrary shaped particle (prolate spheroid in our case) is correct upto O(ReSl).

The perturbation parameter was chosen to be Reynolds number, Re. The hydrodynamic force expression for an arbitrary shaped particle given by Lovalenti and Brady is valid up to O(Re).

Hence, the perturbed solution upto O(Re) was expressed as follows

$$U_P = U_0 + U_1 Re^{1/2} + U_2 Re + O(Re)$$

where,

$$U_0 = \frac{Re_F \sin(t)}{6\pi(cof)}$$

$$U_1 = \frac{QU_0}{6\pi(cof)}\left[\frac{1}{\sqrt{t}} - \frac{1}{\sqrt{\epsilon}}\right] + \frac{3Re_F(Sl\pi)^{1/2}}{(6\pi)^2}\int_0^{t-\epsilon}\frac{\sin(s)}{(t-s)^{3/2}}ds$$

$$U_2 = \frac{-1}{6\pi(cof)}\left\{\frac{c_1 Re_F \cos(t)}{6\pi(cof)} - QU_1\left[\frac{1}{\sqrt{t}} - \frac{1}{\sqrt{\epsilon}}\right] - 3(Sl\pi)^{1/2}(cof)^2\int_0^{t-\epsilon}\frac{U_1(s)}{(t-s)^{3/2}}ds\right\}$$

wherein $Q = 6(Sl\pi)^{1/2}(cof)^2$, $c_1 = \frac{4\pi}{3}\left(\frac{b}{a}\right)^2 + (I_1)Sl$.

The displacement is calculated by numerically integrating the interpolated data of the velocity.

MATLAB was used for computing the above expressions. We found that for low values of Re, typically upto Re=0.2, both the perturbed and the numerical solutions agreed well. Figure 1 shows a comparison between the phase plots obtained by both the methods for aspect ratios 2 and 10, Re=0.1 and ReF = 0.1.

3.3.2 Test 2

When the initial direction of the motion was reversed, namely by replacing ReF with – ReF , the phase space plot was reflected about the zero velocity axis. That is, a reflection of the phase space attractor about the zero velocity axis when the direction of the first motion is reversed was obtained, which can be considered as an important result which demonstrates the correctness of the results.

The results showed a preferred direction in the solution. Since the only physical direction in this problem is the initial direction of the external force, a reversal of that direction should result in a reversal of direction in the solution, which was indeed the case. The tests performed above provide considerable confidence in the results.

4. Results and Discussion

We have four variable parameters in the system; the Reynolds number Re, the Strouhal number Sl, the aspect ratio and the amplitude of the periodic force ReF. It is essential to determine the effect of these parameters on the system. Typical phase space plots (plots of particle velocity vs. position) have been generated for different values

of the Reynolds number, the aspect ratio and the amplitude of the periodic force. In some of the Figures (Figure 3b and Figure 5c), the displacement and velocity values were scaled with their appropriate maximum values obtained in the Stokes' case, i.e. when Re = 0. These values have been termed as displacement and velocity amplitude, respectively. This illuminates the results better so that the individual cases can be compared. One of the parameters was chosen, namely the Strouhal number, a constant and equal to unity. The plots represent an attractor as they are bounded in phase space. Since Sl always occurs in combination with Re, the limit of small Sl number is automatically obtained by reducing Re.

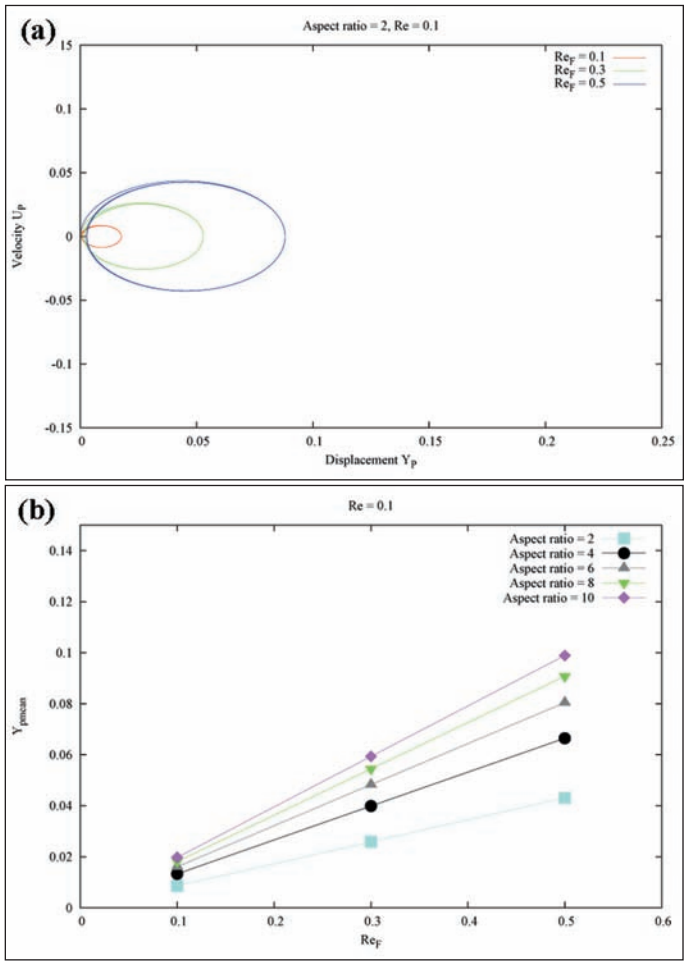

Figure 2. (a) This phase portrait shows the effect of ReF on the system. On increasing the value of ReF, the phase plots get enlarged showing the obvious effect of the forcing term. The phase plots for different ReF values (0.1, 0.3, 0.5), Re=0.1, aspect ratio=2 are superimposed. (b) Plot showing the relationship of Ypmean with ReF.

It was observed that the particle tends to move away from the zero displacement axis with time, i.e. after every cycle, we notice that the mean position is shifted along the displacement axis. This is termed as drift. The average displacement of the particle is determined from the zero-velocity axis and is denoted as Y_{pmean} . There exists a definite relation between Y_{pmean} and Re, as well as Y_{pmean} and Re_F .

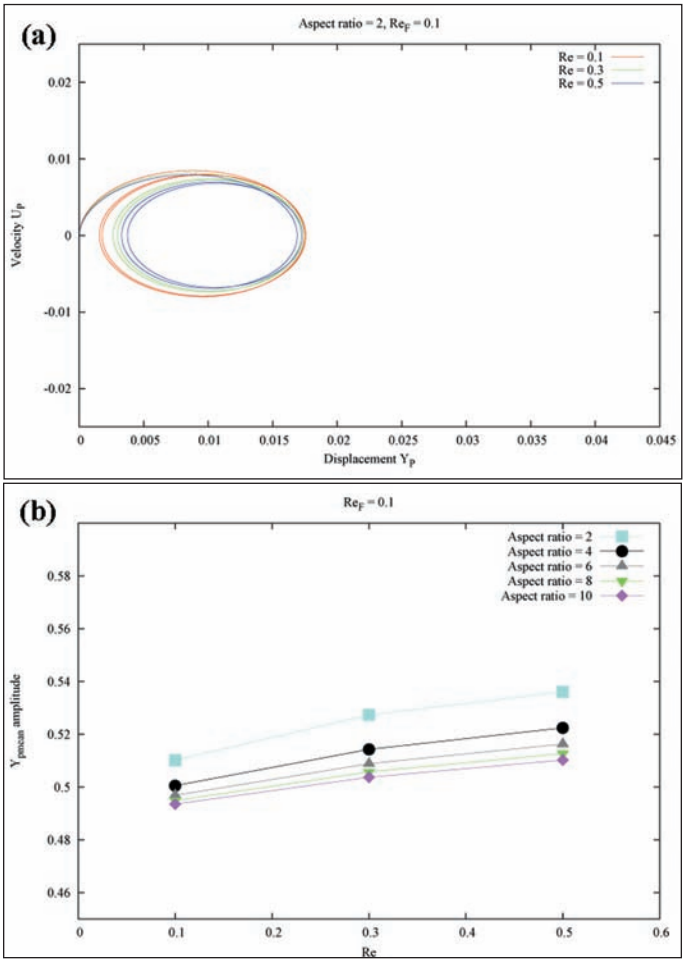

Figure 3. (a) Phase portrait obtained for different Re values (0.1, 0.3, 0.5), ReF=0.1, aspect ratio=2. We can see the effect of increasing Re which results in diminished phase plots. (b) Plot showing the relationship of Ypmean amplitude with Re.

4.1 Effect of Re_F

The area bounded by the phase space plot which is bounded and hence represents an attractor in phase space, increases with increasing amplitude of the forcing term, ReF, establishing the obvious relation between the attractors and the amplitude of the periodic force. As ReF increases, the particle oscillates with larger amplitude and thus covers a larger surface area in the phase plot. As can be seen from the Figure 2(a), the increase in area is quite significant when ReF is increased from 0.1 to 0.5.

4.2 Effect of Re

The effect of increasing the Reynolds number can be seen from Figure 3(a). The effect is opposite compared to that of increasing the amplitude of the forcing term. Increasing Re results in a smaller attractor plot. This shows the effect of inertia on the motion of the particle. Inertial effects dominate at higher Reynolds number and the mean

position of the particle is seen to shift in the direction of initial motion on increasing Re.

4.3 Effect of Aspect Ratio

The values obtained for the acceleration reaction term for different aspect ratios are given in Table 2. The values of the second and third diagonal elements of the tensor are quite similar to one another. This is expected as they both are symmetric to the direction of motion of particle, in the current work. These values provide an idea about the reaction to particle motion and hence the term acceleration reaction. As can be seen, the values decrease with increasing aspect ratio. These values appear in the term Re' in the equation (6). This term additionally contains a factor which is the square of the inverse of aspect ratio. Hence, the effect of this term decreases with increasing aspect ratio. The contribution from the Pseudo-steady Stokes drag also decreases with increasing aspect ratio which again contributes to lower resistance. The lowering of resistance with aspect ratio could be due to the body becoming more streamlined and hence being able to move through the fluid medium easily. Thus, the overall effect of increasing aspect ratio can be seen as an increase in the area bounded by the attractor. The effect of aspect ratio on Y_{pmean} was studied and it was found that Y_{pmean} increases with aspect ratio. This result can be seen in Figure 4.

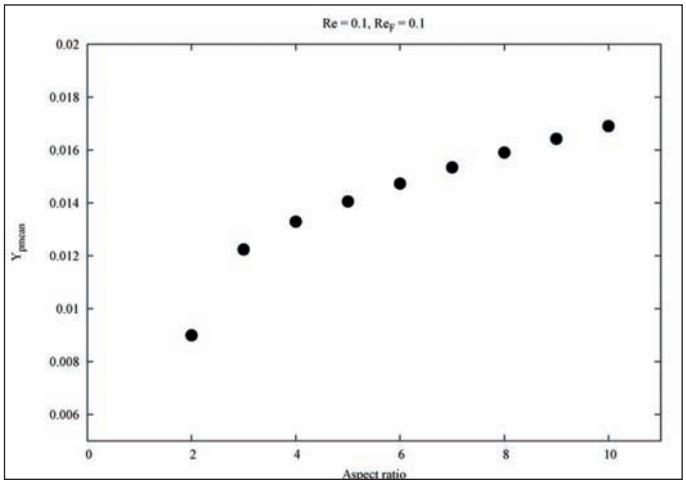

Figure 4. Plot showing the relationship of Ypmean with aspect ratio.

4.4 Effect of Inertia on Steady State

In order to determine the influence of the inertial effects with every cycle, the simulation was run for longer times, typically about 350000 iterations. The phase plots obtained are presented in Figure 5(a,b).

It can be seen that in the initial cycles, the drift is significant when compared to the drift in the later stages of the simulation. Thus, we see that the inertial effects are dominant during the initial stages and later on the particle tends towards an oscillatory steady state. We observe that the inertial effects dominate at lower aspect ratios and their dominance reduces with increasing aspect ratio.

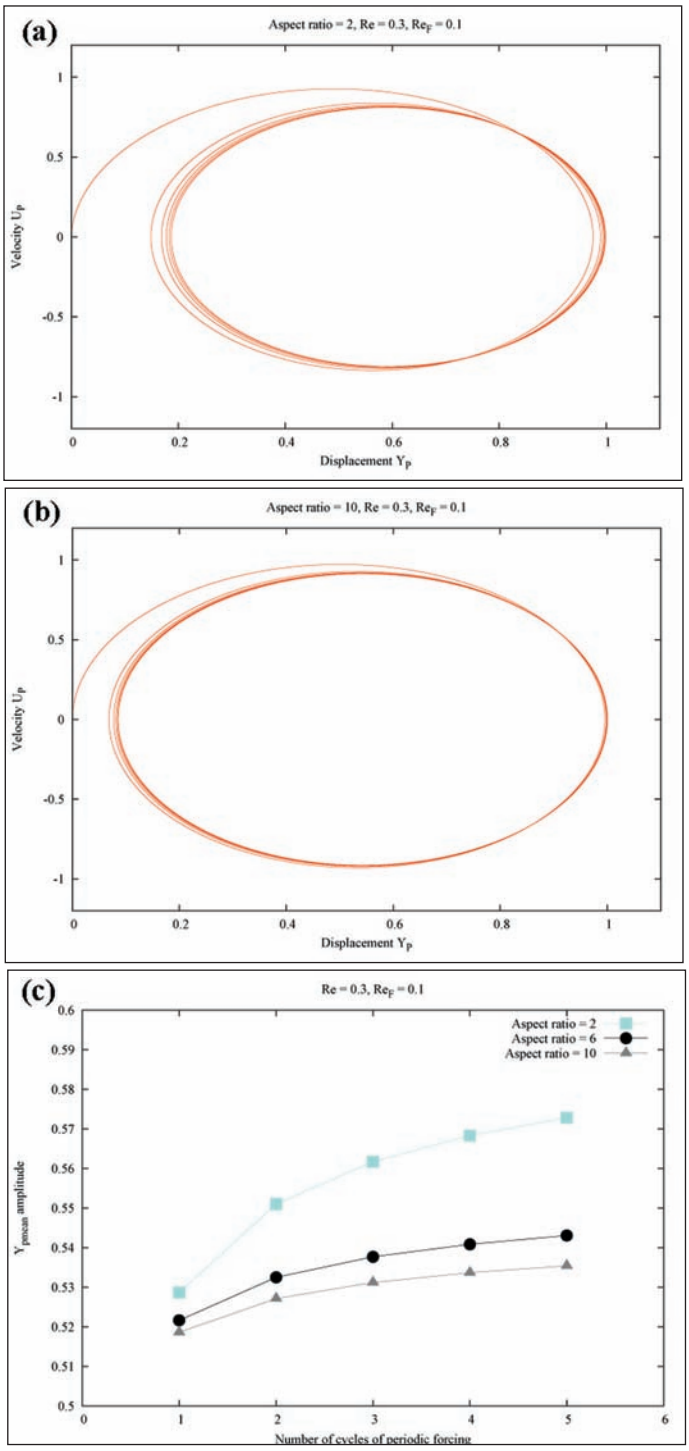

Figure 5. The phase plots obtained for aspect ratio=2 (a) and 10 (b), Re=0.3, ReF=0.1, showing the long time inertial effects and attainment of the steady state. The attainment of the steady state is quicker in (b) as the inertial effects die down quickly due to their relatively insignificant contribution at higher aspect ratios (c) plot showing the drift in mean position with every complete cycle of periodic forcing. Note that the particle attains a steady mean position at longer times.

The attainment of an oscillatory steady state is found to be quicker when the aspect ratio is larger. This happens due to weaker inertial effects. Figure 5(c) shows this effect clearly. Here, we scale Y_{pmean} obtained after every cycle of the periodic forcing term with respect to the maximum displacement obtained in Stokes' case. A steady value of this Y_{pmean} amplitude is attained more quickly when aspect ratio increases.

4.5 Effect of Nonlinearity

The behaviour of the system was analysed by neglecting the unsteady Oseen correction term which contains the non-linear term and compared it with the attractors obtained from the full differential expression (Figure 6).

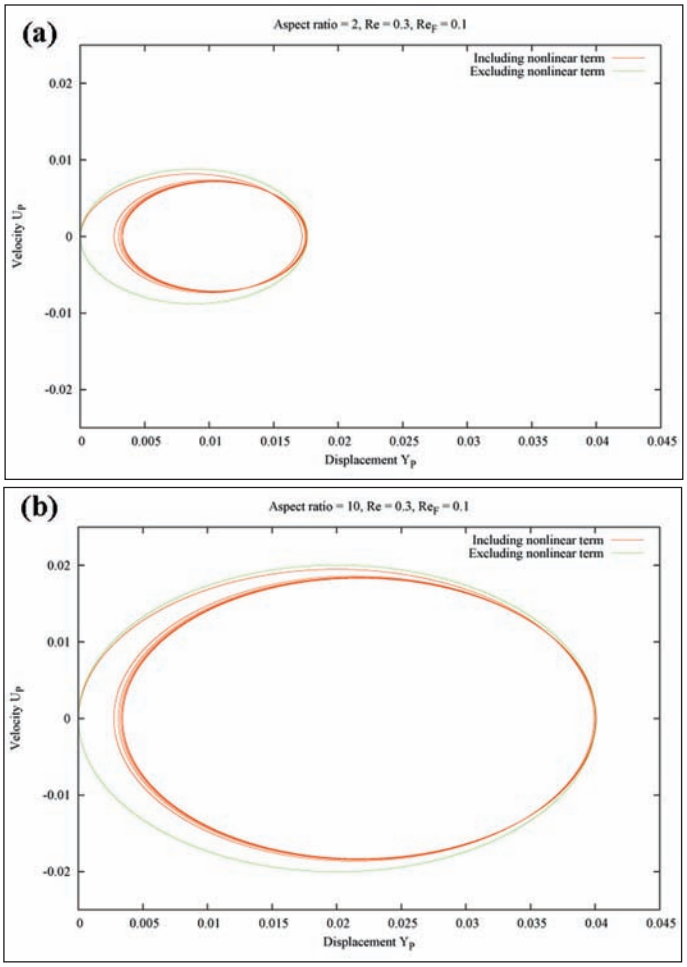

Figure 6. The phase portrait comparing the plots obtained with and without the inclusion of the Oseen correction term and thereby the non-linear term. The effect of inertia on the system can be clearly seen. The non-linear term contribution at higher aspect ratio is reduced and we can see it approaching the curve obtained by neglecting the non-linear term. Here, Re=0.3, ReF=0.1, aspect ratio=2 (a) and 10 (b).

From this, the effects of the non-linear and inertial terms are clear. The phase plots excluding the Oseen correction cover a larger surface area. Another important observation is the absence of drift of the particle from the zero velocity axis. The particle is found to oscillate about a single point. The attainment of steady state is thus strongly dependent on inertia. A slight variation in the parameters considered could vary the inertia and thus approach to steady state.

5. Conclusion

In this paper, an attempt has been made to determine the dynamics of a prolate spheroid under periodic forcing in a quiescent Newtonian fluid medium at low Reynolds numbers. Inertial effects have been included to study the behaviour more realistically. The numerical values for the acceleration reaction term for different aspect ratios were presented. It is observed that these values decrease with increasing aspect ratio.

1. The particle is seen to oscillate under periodic forcing. A preferred direction of motion is observed and it is seen that the particle shows a net displacement along this direction with time.

2. The effect of system variables is studied in detail and it is found that increasing Re restricts the particle motion and hence the size of the attractor.

3. Increasing the periodic force amplitude is found to increase the size of the attractor.

4. The effect of the shape of the particle is studied by varying the aspect ratio. The size of the attractor increases with increasing aspect ratio due to weaker inertial effects.

The results were supplimented with detailed physical arguments and wherever possible, various tests have been conducted to justify the results. The ultimate goal is the rheology, which can be further obtained using the results in this paper, since this will determine the stress deformation behaviour and will determine processing parameters for these suspensions. It is hoped that this work excites further research in this area. Future work could possibly cover 2-D and 3-D aspects of such a motion. It would also be interesting to study the effects of coupling rotation with translation.

Acknowledgements

This work was done at Centre for Mathematical Modelling and Computer Simulation, Bangalore, India, as a part of B.Tech internship. The author would like to acknowledge Dr. T. R. Ramamohan for his continuous guidance. He would like to thank K. Madhukar and Prof. I. S. Shivakumara for their encouragement and Dr. A. R. Upadhya, for his help in taking up this project at National Aerospace Laboratories, Bangalore.

References

[1] L. G. Leal, "Particle motions in a viscous fluid," Annual Reviews in Fluid Mechanics, 1980, 12, 435-476.

[2] G. B. Jeffery, "The motion of ellipsoidal particles immersed in a viscous fluid," Proceedings of the Royal Society of London A, 1922, 102, 161-179.

[3] F. P. Bretherton, "The motion of rigid particles in a shear flow at low Reynolds numbers," Journal of Fluid Mechanics, 1962, 14, 284-304.

[4] G. Subramanian et al., "Inertial effects on the orientation of nearly spherical particles in simple shear flow," 2006, 557, 257-296.

[5] K. Asokan et al., "Review of chaos in the dynamics and rheology of suspensions of orientable particles in simple shear flow subjected to an external periodic force," Journal of Non-Newtonian Fluid Mechanics, 2005, 129, 128-142.

[6] T. R. Ramamohan et al., "Numerical Simulation of the Dynamics of a Periodically Forced Spherical Particle in a Quiescent Newtonian Fluid at Low Reynolds Numbers, Lecture Notes on Computational Science, 2009, 5544, 591-600.

[7] C. V. A. Kumar et al., "Chaotic dynamics of periodically forced spheroids in simple shear flow with potential application to particle separation," Rheologic Acta, 1995, 34, 504-512.

[8] C. V. A. Kumar et al., "Controlling chaotic dynamics of periodically forced spheroids in simple shear flow: results for an example of a potential application," Sadhana, 1998, 23, 131-149.

[9] P. M. Lovalenti et al., "The hydrodynamic force on a rigid particle undergoing arbitrary timedependent motion at small Reynolds number," Journal of Fluid Mechanics, 1993, 256, 561-605.

[10] C. Pozrikidis, "Boundary integral and singularity methods for linearized viscous flow," Cambridge University Press, 1992.

[11] A. T. Chwang et al., "Hydromechanics of low-Reynolds-number flow. Part 2. Singularity method for Stokes flows," Journal of Fluid Mechanics, 1975, 67, 787-815.

[12] T. Tang, "A finite difference scheme for partial integro-differential equations with a weakly singular kernel," Applied Numerical Mathematics, 1993, 11 ,309-319.

[13] G. K. Batchelor, "The stress system in a suspension of force free particles," Journal of Fluid Mechanics, 1970, 41, 545-570.

[14] P. M. Kulkarni et al., "Suspension properties at finite reynolds numbers from simulated shear flow," Physics Fluids, 2008, 20, 040602.

[15] K. Sangtae and S. J. Karrila, "Microhydrodynamics, principles and selected applications," Dover Publications Inc., Mineola, New York, 2005.

[16] Introduction to Perturbation Method, Web link: http://www.sm.luth.se/~tomas/applmath/chap2en/index.html

[17] A. H. Nayfeh, "Perturbation Methods," Wiley Interscience Publication, 1973.

[18] Gradshteyn and Ryzhik, "Table of Integrals," Series and Products, Academic, New York, 1965.

[19] J. D. Lambert, "Computational Methods in Ordinary Differential Equations," Wiley Interscience Publication, 1973.

About the Author

Priyank V. Kumar is an undergraduate student of Metallurgical and Materials engineering at Indian Institute of Technology-Madras, Chennai, India. He joined the department in the month of August, 2006 and is expected to graduate in May 2010. His research interests include Computational Material Sciences, Transport phenomena, Mechanical Metallurgy and Thermodynamics. He has been working on specific topics such as Inertial effects on forced particles at low Reynolds numbers, Molecular Dynamics simulation of Ni/NiAl interfaces, Micromechanical simulation of wear resistant coatings and Computational modelling of Electron Beam Welding process. He has carried out his internship at CSIR Centre for Mathematical modelling and Computer Simulation, Bangalore, India (Summer and Winter '08) and was awarded the DAAD scholarship for his research intern at Institut fur Materialprufung Werkstoffkunde und Festigkeitslehre, University of Stuttgart, Germany (Summer '09). His hobbies include playing cricket, drumming and listening to music.